

OJBKQ: Objective-Joint Babai-Klein Quantization

Xinyu Wang^{1,*}, Ziyu Zhao^{1,*}, Peng Lu², Yu Gu¹, Xiao-Wen Chang¹

¹McGill University

²Université de Montréal

*Equal contribution

{xinyu.wang5, ziyu.zhao2}@mail.mcgill.ca, chang@cs.mcgill.ca,

Abstract

Post-training quantization (PTQ) is widely used to compress large language models without retraining. However, many existing weight-only methods rely on heuristic objectives and greedy rounding, thus leading to noticeable degradation under low-bit quantization. In this work, we introduce OJBKQ (Objective-Joint Babai-Klein Quantization with K-Best Sampling), a layer-wise PTQ method that formulates weight quantization as a joint optimization problem over activations and weights. This formulation results in a multiple-right-hand-side box-constrained integer least squares (BILS) problem in each layer, which is NP-hard. For each column of the weight matrix, we apply an extended Babai nearest-plane algorithm and an extended version of Klein’s randomized Babai algorithm to find the minimum-residual Babai-Klein point, a sub-optimal solution to the BILS problem. Experimental results on large language models show that OJBKQ achieves lower perplexity at 3–4 bits compared to existing PTQ approaches, while maintaining comparable computational cost.

1 Introduction

Large Language Models (LLMs) [Achiam *et al.*, 2023; Touvron *et al.*, 2023; Comanici *et al.*, 2025] pose substantial deployment challenges due to their massive memory footprint and inference costs [Chen *et al.*, 2023]. Layer-wise post-training quantization (PTQ) [Frantar *et al.*, 2023; Lin *et al.*, 2024; Chee *et al.*, 2024] has become a widely adopted compression standard, enabling efficient deployment by sequentially quantizing parameters without retraining. In this work, we focus on standard and practically relevant 4-bit and 3-bit settings (e.g., group size 128) and study how to further improve quantization quality beyond strong PTQ baselines.

Despite its empirical success, layer-wise PTQ is intrinsically a *discrete* optimization problem. At its core, each layer-wise step solves an integer-constrained quadratic subproblem, typically approached with sequential rounding-type solvers. Recent theoretical analyses [Chen *et al.*, 2025] reveal that standard solvers (e.g., GPTQ) admit a lattice-decoding interpretation: they are closely related to Babai’s nearest-plane

algorithm [Babai, 1986], which finds the Babai point, a sub-optimal solution to the Closest Vector Problem (CVP) [Agrell *et al.*, 2002b], which is also referred to as the Integer Least-Squares (ILS) problem. However, when the lattice basis matrix is not well-conditioned or when the dimension is large, the Babai point residual may be much larger than the optimal residual. Thus, we need to find a better sub-optimal solution. Second, minimizing a layer-local proxy loss does not necessarily translate to better end-to-end quantization due to error propagation and input distribution drift; consequently, the *selection objective* used to compare and choose among candidates is as crucial as the solver itself, yet remains inconsistent across methods.

We propose **OJBKQ** (Objective-Joint Babai-Klein Quantization), a unified framework that addresses both issues. **(i) Joint Target Alignment (JTA):** To better align layer-wise decisions with end-to-end behavior under error propagation, we introduce a unified candidate *scoring* objective (Eq. 7) with a single continuous knob. JTA interpolates between two fundamental alignment targets: matching the *runtime* quantized activations induced by the partially-quantized network, and matching the corresponding *full-precision reference* outputs [Arai and Ichikawa, 2025]. The formulated quantization problems at each layer are multiple-right-hand-side box-constrained integer least squares (BILS) problems. **(ii) Random- K quantization:** For each column of the weight matrix in a BILS problem, we apply the box-constrained Babai algorithm to obtain one sub-optimal solution (a low-bit vector candidate). For the same column, we then extend Klein’s K -time randomized Babai algorithm [Klein, 2000] to the box-constrained case to generate K additional sub-optimal solutions independently. Among these $K + 1$ candidates, we select the one which has the minimum residual, referred to as the best Babai-Klein point. There are two levels of parallelization. One across the columns of the weight matrix and the other across the K points produced by the box-constrained Klein algorithm. Both can be implemented efficiently.

In OJBKQ, Random- K expands the quality of the *candidate set*, while JTA improves *how we select* the optimal candidate.

Our contributions are summarized as follows:

- **Quantization Formulation.** We revisit layer-wise PTQ from a CVP perspective and reformulate it as an explicit

lattice-decoding problem. This enables a faithful Babai-style implementation that operates via triangular factors and back-substitution, without materializing any matrix inverse.

- **Superior Sub-optimal Solution.** We extend Klein’s randomized algorithm to the box-constrained case and apply it to PTQ. By running K independent probabilistic traces in parallel, our method explores non-orthogonal lattice bases to find superior integer candidates while maintaining strong language modeling performance with low perplexity in both 4-bit and 3-bit configurations. In designing and implementation of our numerical algorithm, we take both accuracy and efficiency into account. For example, unlike GPTQ, no inverse of a matrix is computed. To reduce the computational overhead of multiple independent solution, we design a GPU-efficient algorithm presented in Appendix A
- **JTA Candidate Selection.** We propose the **Joint Target Alignment (JTA)** objective, a unified scoring criterion that subsumes commonly used PTQ objectives as special cases by varying the alignment target between runtime-quantized and full-precision references, providing a more fine-grained criterion for candidate selection under error propagation.

2 Related Work

Layer-wise post-training quantization (PTQ). Post-training quantization is a practical standard for compressing large language models without retraining. Following recent PTQ taxonomies [Zhao *et al.*, 2025], mainstream weight-only PTQ methods can be broadly grouped by their dominant mechanism. *Compensation-based* approaches, exemplified by GPTQ [Frantar *et al.*, 2023], quantize weights sequentially while updating the remaining unquantized weights to compensate for accumulated quantization errors, often leveraging second-order curvature surrogates estimated from calibration data. *Rotation-based* methods such as QuIP [Chee *et al.*, 2024] apply structured transformations to reshape weight distributions and improve quantizability under low-bit constraints. *Saliency-based* methods, represented by AWQ [Lin *et al.*, 2024], reduce quantization error by selecting scaling factors according to activation/weight importance, avoiding mixed-precision deployment. In addition, *optimization-based* approaches (e.g., OmniQuant¹ and PoTPTQ) [Shao *et al.*, 2024; Wang *et al.*, 2025] directly optimize quantization parameters with lightweight objectives while keeping pretrained weights frozen. Overall, existing PTQ pipelines mainly differ along two orthogonal axes: (i) the approximate *solver* used to handle the discrete subproblem, and (ii) the *objective* used to evaluate candidates and guide selection.

Integer least squares and Babai-type solution. The integer least squares (ILS) problems or/and its box-constrained

¹Although it is classified as PTQ in the survey, it still requires training on the calibration dataset to find scales. Then we exclude it from our baselines

variant (BILS) arise in cryptograph [Micciancio and Goldwasser, 2002], GPS [Teunissen, 1996; Chang *et al.*, 2005, 2023], MIMO detection [Agrell *et al.*, 2002a; Bai *et al.*, 2014] etc, where the goal is to recover a discrete-valued vector under a quadratic objective. Since the ILS and BILS are NP-hard [Micciancio, 2002; Verdú, 1989], in some application often efficient sub-optimal solutions are applied. An often used method is Babai’s nearest-plane algorithm [Babai, 1986], which computes the Babai point by back substitution on an upper-triangular linear system, where rounding is performed at each step. The Babai point is the first integer point found by the Schnorr–Euchner sphere-decoding algorithm, which enumerates integer points in an ellipsoid to find the optimal solution [Schnorr and Euchner, 1994]. It has been extended to the box-constrained case [Wen and Chang, 2021]. While computationally efficient, when the coefficient matrix (referred to as the lattice basis matrix in lattice theory) is not well-conditioned (or not well-reduced in lattice theory), or when the dimension of the integer vector is large. There are other sub-optimal algorithms, such as those proposed in [Barbero and Thompson, 2006; Chang *et al.*, 2024], but they are not suitable for GPU computing. Fortunately, there is a randomized version of the Babai algorithm proposed in [Klein, 2000], which is not widely used yet. In each step of the Babai algorithm, Klein’s algorithm rounds the real solution to a nearby integer according to a predefined distribution. When the algorithm is called K times, it generates K points. Then the best one, which gives the minimum residual, is chosen as the final sub-optimal solution. This method can be parallelized. The method is for unconstrained ILS problem and has not been widely used yet. Recently, the connection between sequential PTQ solvers and the Babai point has gained attention [Chen *et al.*, 2025]. This paper emphasizes that the PTQ problems can be modeled as BILS problems so that sub-optimal BILS algorithms can be applied.

Objectives under error propagation and distribution drift. A recurring challenge in layer-wise PTQ is that minimizing a layer-local reconstruction proxy does not necessarily translate to improved end-to-end quality, due to quantization error propagation and the resulting input distribution drift across layers. Consequently, the choice of the *alignment target*—whether to match outputs under runtime (partially-quantized) activations or to match full-precision reference outputs—plays a central role in practical PTQ performance. Recent work revisits this issue from an error-propagation viewpoint and advocates objectives that better reflect downstream behavior under partial quantization [Arai and Ichikawa, 2025]. Our JTA objective follows this perspective but provides a unified scoring criterion with a single continuous knob that interpolates between runtime-quantized activations and full-precision reference targets, enabling consistent candidate selection across layers.

3 Methodology

3.1 Layer-wise Objectives and Joint Target Alignment (JTA)

We now start analyze commonly used layer-wise PTQ objectives. Consider a linear layer with full-precision weight

matrix $\mathbf{W} \in \mathbb{R}^{m \times n}$. Let $\mathbf{X} \in \mathbb{R}^{p \times m}$ be full-precision calibration activations, $\tilde{\mathbf{X}} \in \mathbb{R}^{p \times m}$ be the corresponding *runtime* activations produced by a partially quantized network (i.e., upstream layers already quantized), $\mathbf{Y}^{\text{fp}} := \mathbf{X}\mathbf{W}$ denote the full-precision reference output, and $\mathbf{Y}^{\text{rt}} := \tilde{\mathbf{X}}\mathbf{W}$ denote the runtime-consistent reference output under partially quantized activations. At runtime, a candidate $\widehat{\mathbf{W}}$ produces the output $\widehat{\mathbf{Y}} := \tilde{\mathbf{X}}\widehat{\mathbf{W}}$.

Many existing objectives can be interpreted as choosing different alignment targets:

$$\text{(Runtime-consistent)} \quad \min_{\widehat{\mathbf{W}}} \|\tilde{\mathbf{X}}\widehat{\mathbf{W}} - \tilde{\mathbf{X}}\mathbf{W}\|_F^2 \quad (1)$$

$$= \|\widehat{\mathbf{Y}} - \mathbf{Y}^{\text{rt}}\|_F^2, \quad (2)$$

$$\text{(Full-precision mapping)} \quad \min_{\widehat{\mathbf{W}}} \|\mathbf{X}\widehat{\mathbf{W}} - \mathbf{X}\mathbf{W}\|_F^2, \quad (3)$$

$$\text{(Mismatch target)} \quad \min_{\widehat{\mathbf{W}}} \|\tilde{\mathbf{X}}\widehat{\mathbf{W}} - \mathbf{X}\mathbf{W}\|_F^2 \quad (4)$$

$$= \|\widehat{\mathbf{Y}} - \mathbf{Y}^{\text{fp}}\|_F^2. \quad (5)$$

Eq. (1) directly reflects runtime behavior but aligns to a target computed on quantized activations, which may be noisy; this objective is adopted by GPTQ and QUIP. Eq. (3) admits a convenient least-squares structure (prior to discretization) but suffers from train-run mismatch when earlier layers are quantized, and is optimized by AWQ. Eq. (4) partially alleviates this mismatch by evaluating candidates on runtime activations while preserving the full-precision reference; QEP employs this objective as a corrective patch within a layer-wise quantization pipeline, although it may over-penalize candidates when error drift accumulates across layers.

These trade-offs motivate a unified selection objective that interpolates between runtime-consistent and full-precision references, while optionally controlling weight drift.

We propose an expressive *Joint Target Alignment (JTA)* objective with a single continuous knob to score and select candidates generated by Random- K decoding. We define an interpolated target

$$\mathbf{Y}^*(\mu) := (1 - \mu)\mathbf{X}\mathbf{W} + \mu\tilde{\mathbf{X}}\mathbf{W}, \quad \mu \in [0, 1], \quad (6)$$

and formulate the ILS problem:

$$\min \mathcal{S}(\widehat{\mathbf{W}}) := \|\tilde{\mathbf{X}}\widehat{\mathbf{W}} - \mathbf{Y}^*(\mu)\|_F^2 + \lambda^2 \|\widehat{\mathbf{W}} - \mathbf{W}\|_F^2, \quad (7)$$

where $\widehat{\mathbf{W}}$ is subject to some constraint. Later we will show this is a multiple-right-hand-side box-constrained integer least squares (BILS) problem and provide a sub-optimal solution. The knob μ interpolates between matching full-precision and runtime-consistent references, while λ optionally regularizes weight displacement. In our framework, **Random- K quantization** (Sec. 3.4) rewrites find a sub-optimal solution to , and **JTA** (Eq. (7)) provides a consistent curvature-aware criterion for selecting the best candidate under error propagation. When $\mu=1$ and $\lambda=0$, Eq. (7) reduces to the runtime-consistent objective in Eq. (1); when $\mu=0$ and $\lambda=0$, it aligns to the full-precision reference in Eq. (4).

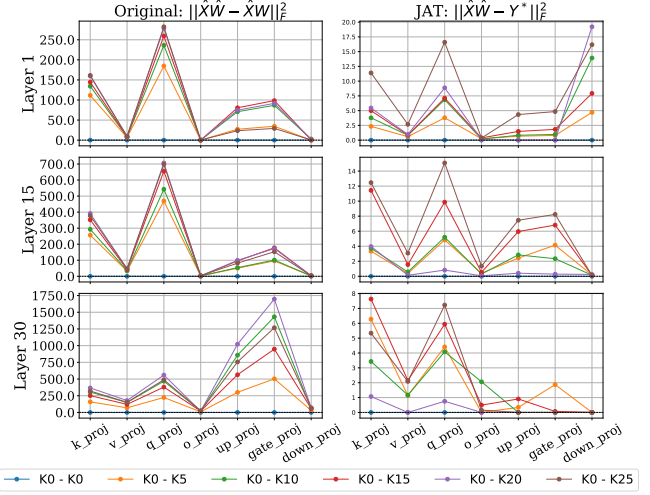


Figure 1: Layer-wise comparison of the original output norms and JTA reconstruction errors across Layers 1, 15, and 30. We present results for all linear modules under varying K settings.

End-to-end layer-wise procedure. For each layer, we (i) form $\tilde{\mathbf{X}}$ by a partially quantized forward pass, (ii) find a sub-optimal optimal solution to Eq. (7), to be seen in the next sections. This closes the loop between discrete candidate generation and objective-aligned selection.

3.2 From Layer-wise Quantization to Integer Least Squares

From (7) we obtain

$$\mathcal{S}(\widehat{\mathbf{W}}) := \left\| \begin{bmatrix} \tilde{\mathbf{X}} \\ \lambda \mathbf{I} \end{bmatrix} \widehat{\mathbf{W}} - \begin{bmatrix} \mathbf{Y}^*(\mu) \\ \lambda \mathbf{W} \end{bmatrix} \right\|_F^2. \quad (8)$$

The task of finding an optimal quantized weight $\widehat{\mathbf{W}}$ to minimize the selection objective in Sec. 3.1 can be formally mapped to the classical *Integer Least Squares* (ILS) problem.

To facilitate the derivation, we first introduce additional notation. Let

$$\mathbb{B} = \{0, 1, \dots, 2^{\text{wbit}} - 1\}$$

denote the box constraint corresponding to the set of admissible integer values for a wbit-bit quantized weight. Let

$$\mathbf{Q} = [\mathbf{q}_1, \mathbf{q}_2, \dots, \mathbf{q}_n] \in \mathbb{B}^{m \times n}$$

denote the quantized version of the full-precision weight matrix \mathbf{W} . We further define

$$\mathbf{S} = [\mathbf{s}_1, \mathbf{s}_2, \dots, \mathbf{s}_n] \in \mathbb{R}^{m \times n}, \quad \mathbf{Z} = [\mathbf{z}_1, \mathbf{z}_2, \dots, \mathbf{z}_n] \in \mathbb{R}^{m \times n}$$

as the scale matrix and zero-point matrix, respectively. Both \mathbf{S} and \mathbf{Z} are pre-computed using standard statistical calibration methods (e.g., the Absmax method).

Finally, the dequantized weight matrix is given by

$$\widehat{\mathbf{W}} = \mathbf{S} \odot (\mathbf{Q} - \mathbf{Z}),$$

where \odot denotes element-wise multiplication. The matrices \mathbf{Q} , \mathbf{S} , \mathbf{Z} , and $\widehat{\mathbf{W}}$ are all partitioned column-wise in the same manner as \mathbf{W} . We further define

$$\mathbf{A} := \begin{bmatrix} \tilde{\mathbf{X}} \\ \lambda \mathbf{I} \end{bmatrix}, \quad \mathbf{T} := \begin{bmatrix} \mathbf{Y}^*(\mu) \\ \lambda \mathbf{W} \end{bmatrix}.$$

Using the above notation, Eq. (8) can be rewritten as

$$\sum_{j=1}^n \|\mathbf{A}\mathbf{D}_j\mathbf{q}_j - \mathbf{b}_j\|_2^2,$$

where $\mathbf{D}_j = \text{diag}(\mathbf{s}_j) \in \mathbb{R}^{m \times m}$ is a diagonal scaling matrix, and

$$\mathbf{b}_j = \mathbf{t}_j + \mathbf{A}\mathbf{D}_j\mathbf{z}_j$$

with \mathbf{t}_j denoting the j -th column of \mathbf{T} .

As a result, Eq. (8) decomposes into n independent box-constrained integer least squares (BILS) problems:

$$\min_{\mathbf{q}_j \in \mathbb{B}^m} \|\mathbf{A}\mathbf{D}_j\mathbf{q}_j - \mathbf{b}_j\|_2^2, \quad j = 1, \dots, n. \quad (9)$$

Since each subproblem is independent, we simplify notation by focusing on a single per-column subproblem:

$$\min_{\mathbf{q} \in \mathbb{B}^m} \|\mathbf{A}\mathbf{D}\mathbf{q} - \mathbf{b}\|_2^2. \quad (10)$$

Solving Eq. (10) exactly is NP-hard for general lattices [Micciancio, 2002]. A classical and efficient approximation is given by the *Babai point* [Babai, 1986], which performs successive orthogonal projections followed by greedy rounding along a triangular factorization of \mathbf{A} . It matches the recent analyses [Chen *et al.*, 2025] which suggest that layer-wise solvers such as GPTQ can be interpreted as greedy lattice decoding methods under alternative objective formulations. While the objectives may differ, the underlying principle—approximating a structured lattice decoding problem—remains the same.

3.3 Babai-Based Quantization

Define $\bar{\mathbf{A}} := \mathbf{A}\mathbf{D}$. Then Eq. (10) can be rewritten as the box-constrained integer least squares (ILS) problem

$$\min_{\mathbf{q} \in \mathbb{B}^m} \|\bar{\mathbf{A}}\mathbf{q} - \mathbf{b}\|_2^2. \quad (11)$$

Let $\bar{\mathbf{q}} \in \mathbb{R}^m$ denote the unconstrained real least-squares solution of Eq. (11). The corresponding normal equations are given by

$$\mathbf{D}\mathbf{A}^\top \mathbf{A}\mathbf{D}\bar{\mathbf{q}} = \mathbf{D}\mathbf{A}^\top \mathbf{b} = \mathbf{D}\mathbf{A}^\top (\mathbf{y} + \mathbf{A}\mathbf{D}\mathbf{z}).$$

Rearranging terms yields

$$\mathbf{A}^\top \mathbf{A}\mathbf{D}(\bar{\mathbf{q}} - \mathbf{z}) = \mathbf{A}^\top \mathbf{y}.$$

Let $\mathbf{A}^\top \mathbf{A} = \mathbf{R}^\top \mathbf{R}$ be the Cholesky factorization, where \mathbf{R} is upper triangular. Substituting this factorization into Eq. (3.3) gives

$$\mathbf{R}^\top \mathbf{R}\mathbf{D}(\bar{\mathbf{q}} - \mathbf{z}) = \mathbf{A}^\top \mathbf{y}.$$

Define the transformed variable

$$\mathbf{v} := \mathbf{D}(\bar{\mathbf{q}} - \mathbf{z}),$$

which implies

$$\bar{\mathbf{q}} = \mathbf{D}^{-1}\mathbf{v} + \mathbf{z} = \mathbf{v} \oslash \mathbf{s},$$

where \oslash denotes element-wise division.

Finally, define $\bar{\mathbf{R}} := \mathbf{R}\mathbf{D}$. It is straightforward to verify that Eq. (11) is equivalent to

$$\min_{\mathbf{q} \in \mathbb{B}^m} \|\bar{\mathbf{R}}(\mathbf{q} - \mathbf{z}) - \mathbf{R}^{-\top} \mathbf{A}^\top \mathbf{y}\|_2^2, \quad (12)$$

which admits efficient approximate solutions via Babai-type successive rounding.

Algorithm 1 Quantization with JTA

- 1: Compute \mathbf{s} and \mathbf{z}
 - 2: Compute the Cholesky factorization: $\tilde{\mathbf{X}}^\top \tilde{\mathbf{X}} + \lambda^2 \mathbf{I} = \mathbf{R}^\top \mathbf{R}$
 - 3: Solve the lower triangular system $\mathbf{R}^\top \mathbf{u} = \mathbf{A}^\top \mathbf{y}$ and the upper triangular system $\mathbf{R}\mathbf{v} = \mathbf{u}$.
 - 4: Compute $\bar{\mathbf{q}} = \mathbf{v} \oslash \mathbf{s} + \mathbf{z}$
 - 5: Compute $\bar{\mathbf{R}} = \mathbf{R}\mathbf{D}$
 - 6: $\mathbf{c}(m) = \hat{\mathbf{q}}(m)$
 - 7: $\mathbf{q}(m) = \text{clamp}(\lfloor \mathbf{c}(m) \rfloor; \mathbb{B})$
 - 8: **for** $i = m - 1 : -1 : 1$ **do**
 - 9: $\mathbf{c}(i) = \bar{\mathbf{q}}(i) + \left(\sum_{j=i+1}^m \bar{\mathbf{R}}(i, j)(\bar{\mathbf{q}}(j) - \mathbf{q}(j)) \right) / \bar{\mathbf{R}}(i, i)$
 - 10: $\mathbf{q}(i) = \text{clamp}(\lfloor \mathbf{c}(i) \rfloor; \mathbb{B})$
 - 11: **end for**
-

3.4 Random- K Babai/Klein Decoding (Candidate Generation)

However, as previously mentioned, the Babai algorithm typically produces a suboptimal solution due to its greedy rounding strategy, which does not fully explore the combinatorial structure of the underlying lattice. To address this limitation, Klein [Klein, 2000] proposed a randomized integer least squares (ILS) solver that introduces controlled randomness into the rounding process, enabling the algorithm to explore a richer set of lattice points while maintaining polynomial-time complexity.

Klein-style randomized rounding. In each back-substitution step, instead of deterministic rounding such as the line 6 or 10 in Algorithm 1, we sample \mathbf{q}_i from a distribution concentrated around c_i :

$$\Pr(\mathbf{q}_i = v) = \frac{\exp(-\alpha \bar{\mathbf{R}}_{ii} (\mathbf{c}_i - v)^2)}{\sum_{u=0}^{Q_{\max}} \exp(-\alpha \bar{\mathbf{R}}_{ii} (\mathbf{c}_i - u)^2)}, \quad v \in \mathcal{B}, \quad (13)$$

where $\alpha > 0$ controls the sampling temperature. Larger α approaches greedy Babai; smaller α encourages exploration. When $K=1$ and $\alpha \rightarrow \infty$, the method reduces to deterministic Babai. To further enhance performance, we are inspired by the *K-best Klein* strategy. Specifically, the randomized Klein algorithm is executed independently for K trials, each producing a candidate integer solution. Among these K candidates, we select the one that minimizes the corresponding residual, yielding a more accurate approximation to the underlying integer least squares objective. See Figure 1 on the performance. For this paper, we followed [Liu *et al.*, 2011] design choices where $\alpha = \ln(\rho) / \min_{1 \leq i \leq m} r_{ii}^2$ and ρ is the solution of $K = (e\rho)^{(2m/\rho)}$. This formulation yields a data-driven trade-off between exploration and exploitation, adaptively adjusting the sampling sharpness according to the lattice geometry and the target list size K .

Reference greedy path. We reserve a reference path that uses deterministic rounding, guaranteeing inclusion of the Babai solution in the candidate set.

GPU-efficient Path-Isolated Random- K Babai Search

Naively parallelizing K decoding paths on GPU can introduce *cross-path interference* when residual states are shared

| | Method | L2-7B | L2-13B | L3-8B | Q3-0.6B | Q3-4B | Q3-8B | M-7B |
|-----------------------------|---------|-------------------|------------------|-------------------|--------------------|--------------------|--------------------|------------------|
| | BF16 | 6.97/5.47 | 6.47/4.88 | 8.93/6.13 | 25.28/20.94 | 16.53/13.67 | 13.23/9.72 | 8.15/5.50 |
| g128 W4A16 | RTN | 7.72/6.11 | 6.83/5.20 | 12.09/8.53 | 42.20/37.52 | 20.15/17.52 | 15.54/11.97 | 8.96/6.12 |
| | GPTQ | 7.11/5.62 | 6.56/4.99 | 9.41/6.54 | 30.79/25.20 | 16.73/13.66 | 13.51/10.08 | 8.29/5.63 |
| | AWQ | 7.16/ 5.61 | 6.56/4.97 | 9.40/6.54 | 27.99/25.89 | 17.18/18.43 | 13.51/10.02 | 8.28/5.61 |
| | Ours(N) | 7.15/5.63 | 6.56/4.99 | 9.38/6.52 | 28.35/23.48 | 18.20/13.97 | 13.42/9.97 | 8.27/5.60 |
| | Ours(R) | 7.14/5.62 | 6.55/4.98 | 9.35/6.50 | 28.07/23.64 | 16.44/13.84 | 13.40/9.95 | 8.27/5.59 |
| | Ours | 7.14/5.61 | 6.55/4.97 | 9.33/6.48 | 26.84/22.80 | 16.32/13.54 | 13.39/9.94 | 8.23/5.58 |
| g128 W3A16 | RTN | 4e2/5e2 | 12.50/10.68 | 4e2/2e3 | 1e5/2e5 | 3e3/3e3 | 5e2/7e2 | 19.65/14.88 |
| | GPTQ | 7.92/6.44 | 6.99/5.43 | 12.25/8.35 | 43.60/41.54 | 18.16/15.19 | <u>14.34/11.01</u> | 9.10/6.27 |
| | AWQ | 7.90/ 6.25 | 6.95/5.33 | 11.63/8.19 | <u>39.60/36.88</u> | 19.75/16.83 | 14.97/11.23 | 8.89/6.07 |
| | Ours(N) | 7.88/6.33 | 6.98/5.41 | 11.52/8.19 | 47.23/42.75 | 25.46/20.36 | 14.44/11.11 | <u>8.87/6.06</u> |
| | Ours(R) | 7.87/6.34 | 6.94/5.39 | 11.43/8.16 | 44.09/40.19 | <u>19.52/14.91</u> | 14.37/11.05 | 8.86/6.03 |
| | Ours | 7.86/6.30 | 6.94/5.33 | 11.40/7.87 | 35.03/31.75 | 17.01/12.89 | 14.30/10.98 | 8.84/6.03 |
| W4A16 | GPTQ | 7.37/5.83 | 6.70/5.16 | 10.30/7.37 | 37.03/33.64 | 17.34/14.34 | 13.99/10.65 | 8.53/5.81 |
| | AWQ | 7.34/5.83 | 6.68/5.06 | 9.44/7.10 | 30.07/25.89 | 18.83/16.35 | 14.29/10.77 | 10.24/5.88 |
| | QUIP | 12.54/10.44 | 6.71/5.15 | 9.84/6.85 | 51.41/47.10 | 182.16/126.55 | 19.19/14.85 | 9.69/6.65 |
| | Ours(N) | 7.14/5.64 | 6.57/4.98 | 9.39/6.52 | 28.35/23.48 | 17.30/14.30 | 13.41/9.97 | 8.28/5.62 |
| | Ours(R) | 7.11/5.62 | 6.56/4.97 | 9.38/6.50 | 28.11/23.04 | 17.30/14.30 | 13.41/9.96 | 8.27/5.60 |
| | Ours | 7.10/5.60 | 6.56/4.96 | 9.33/6.48 | 26.94/22.61 | 17.25/14.27 | 13.38/9.92 | 8.24/5.59 |
| W3A16 | GPTQ | 9.83/8.33 | 8.04/6.52 | 29.42/23.81 | 90.23/90.98 | 23.16/21.39 | 18.10/16.46 | 10.90/8.01 |
| | AWQ | 15.62/15.51 | 8.17/6.45 | 17.60/11.84 | 78.52/79.44 | 30.31/33.19 | <u>18.36/14.97</u> | 10.27/7.65 |
| | QUIP | 27.47/28.05 | 7.17/5.57 | 11.50/8.31 | 121.26/112.09 | 23.02/19.74 | 30.39/19.78 | 9.30/6.61 |
| | Ours(N) | 7.88/6.30 | 6.97/5.42 | 11.52/8.17 | 47.23/42.75 | 22.95/19.65 | 25.46/20.36 | 8.78/6.09 |
| | Ours(R) | 7.87/6.29 | 6.97/5.41 | 11.35/8.12 | 43.94/39.77 | 22.90/19.63 | 18.07/16.48 | 8.77/6.07 |
| | Ours | 7.75/6.22 | 6.96/5.40 | 11.38/8.04 | 35.56/32.95 | 22.87/19.56 | 18.05/14.75 | 8.72/6.06 |

Table 1: Perplexity comparison across different models and quantization methods. For each entry, the left value is evaluated on C4 and the right value on WikiText-2. We denote our proposed methods as follows: **Ours(N)** represents Naïve Babai, **Ours(R)** represents Random- K Babai, and **Ours** represents Random- K Babai with Joint Activation-Target optimization. The model families are abbreviated as: L2/L3 for the Llama2/Llama 3, Q3 for the Qwen3 series, and M for Mistral. All activations are in BF16 format.

or updated in-place after paths diverge, leading to incorrect centers c_i and biased sampling. We introduce a GPU-efficient random K -best Babai solver with strict path isolation, termed **Parallel Path-Isolated K -best Babai (PPI-KBabai)** (or **Path-Isolated Random- K Babai Search**). Unlike naive parallel K -path implementations that share residual states, our method maintains an independent residual buffer per candidate path and performs blocked look-ahead updates via batched matrix multiplication. We further reserve a reference greedy path to guarantee inclusion of the deterministic Babai solution, and select the best candidate using the unified JTA score in Sec. 3.1. The Klein Styled JTA quantization, K-Best JTA quantization and detailed kernel design, buffer layout, and blocked update rules are provided in Appendix A.

4 Experiments

To evaluate the effectiveness of our method, we conduct comprehensive experiments comparing it against commonly used layer-wise quantization baselines. We first describe the baseline methods, the large language models being quantized, as well as the evaluation metrics and datasets. We then present the experimental results, followed by a detailed analysis. To ensure fair comparisons, we adopt the default configurations of each baseline’s repo whenever possible.

Baselines We evaluate our method against state-of-the-art quantization approaches, including AWQ [Lin *et al.*, 2024], GPTQ [Chen *et al.*, 2023], and QUIP [Chee *et al.*, 2024], and additionally report round-to-nearest as a naïve base-

line for perplexity. Our method is evaluated under three settings: Naïve Babai (Ours-N), Random- K Babai (Ours-R), and Random K Babai with Joint Activation-Target optimization (Ours). Although theoretically, the K can be any positive integer number, considering the trade-off between resource usage and performance gain Figure 2, we set the K as 5 in our experiments. To ensure strong baselines, we enable activation ordering for GPTQ. Calibration is performed using 128 samples from the C4 [Raffel *et al.*, 2020a] dataset with a sequence length of 2048 tokens. For all baselines, only minimal modifications are made to accommodate the architectural structures of newer LLMs, while their original algorithms and configurations are kept unchanged.

Models We consider two major LLM families, Qwen [Yang *et al.*, 2025] and LLaMA [Touvron *et al.*, 2023; Grattafiori *et al.*, 2024], together with Mistral-7B [Jiang *et al.*, 2023]. This selection covers diverse model families, reasoning capabilities, and parameter sizes.

Metrics and Datasets To test the basic text generation ability, we use the perplexity to measure each quantized model on C4 [Raffel *et al.*, 2020a] and Wikitext2 [Raffel *et al.*, 2020b]. Then we further evaluate on the zero shot accuracy on ARC [Clark *et al.*, 2018], boolq [Wang *et al.*, 2019], HellaSwag [Zellers *et al.*, 2019], PIQA [Bisk *et al.*, 2020] and WinoGrande [Sakaguchi *et al.*, 2021]. For the last part, we test the reasoning ability on GSM-8K [Cobbe *et al.*, 2021], GPQA-diamond [Rein *et al.*, 2023] and MBPP [Austin *et al.*, 2021]. Except the evaluation of PPL, all other tasks are evalu-

| Model | Method | 4 bits | | | | | | | 3 bits | | | | | | |
|-----------|--------|--------------|--------------|--------------|--------------|--------------|--------------|--------------|--------------|--------------|--------------|--------------|--------------|--------------|--------------|
| | | ARC-C | ARC-E | BoolQ | Hella | PIQA | Wino | Average* | ARC-C | ARC-E | BoolQ | Hella | PIQA | Wino | Average* |
| Llama3-8B | BF16 | 51.71 | 80.89 | 81.77 | 60.56 | 78.84 | 73.40 | 71.20 | 51.71 | 80.89 | 81.77 | 60.56 | 78.84 | 73.40 | 71.20 |
| | GPTQ | 48.29 | 78.89 | 80.21 | 59.47 | 78.29 | 73.32 | 69.74 | 34.21 | 66.04 | 71.89 | 55.26 | 73.56 | 68.11 | 61.51 |
| | AWQ | 48.70 | <u>79.21</u> | 80.80 | 59.73 | 78.62 | 73.32 | 70.06 | 43.86 | 75.21 | 76.15 | 55.79 | 75.95 | 71.03 | 66.33 |
| | QUIP | 46.25 | <u>77.36</u> | 81.93 | 58.76 | 77.53 | 73.09 | 69.15 | 41.38 | 71.34 | 77.68 | 55.67 | 76.12 | 71.67 | 65.64 |
| | O(N) | 48.46 | 78.53 | 81.04 | 60.00 | 78.18 | 73.16 | 69.90 | 41.81 | 71.71 | 76.73 | 56.71 | 76.88 | 71.35 | 65.87 |
| | O(R) | 49.32 | 79.12 | 81.04 | <u>59.79</u> | <u>78.24</u> | <u>72.30</u> | <u>69.97</u> | 41.30 | <u>73.48</u> | <u>76.45</u> | <u>56.67</u> | <u>77.37</u> | 70.64 | <u>65.99</u> |
| | O | <u>49.15</u> | 79.59 | <u>81.13</u> | <u>59.70</u> | 78.67 | <u>72.69</u> | 70.16 | <u>42.92</u> | 75.42 | 78.69 | <u>55.73</u> | 77.75 | <u>70.32</u> | 66.81 |
| Qwen3-4B | BF16 | 50.34 | 80.26 | 85.11 | 52.29 | 75.30 | 65.67 | 68.16 | 50.34 | 80.26 | 85.11 | 52.29 | 75.30 | 65.67 | 68.16 |
| | GPTQ | 47.57 | 77.90 | 82.43 | 50.12 | 74.43 | 62.43 | 65.81 | 39.33 | 70.92 | 80.95 | 46.81 | 70.92 | 61.64 | 61.76 |
| | AWQ | 46.29 | 77.32 | 83.23 | 50.37 | <u>74.10</u> | 62.88 | 65.70 | 40.27 | 68.27 | 81.19 | 46.02 | 70.87 | 60.38 | 61.17 |
| | QUIP | 39.25 | 71.09 | 80.73 | 43.64 | 70.24 | 59.91 | 60.81 | 24.15 | 47.81 | 67.86 | 33.72 | 62.79 | 51.14 | 47.91 |
| | O(N) | 41.81 | 74.79 | <u>83.46</u> | 47.61 | 73.12 | 58.33 | 63.19 | 35.95 | 58.68 | 69.20 | 40.65 | 67.74 | 50.83 | 53.84 |
| | O(R) | 44.28 | 74.03 | 82.97 | <u>49.28</u> | <u>72.80</u> | <u>61.17</u> | <u>64.09</u> | <u>37.79</u> | <u>65.35</u> | <u>70.58</u> | <u>43.39</u> | <u>67.25</u> | <u>53.99</u> | <u>56.39</u> |
| | O | 46.65 | 78.27 | 84.31 | 49.85 | 74.21 | 62.35 | 65.94 | 41.50 | 71.41 | 80.95 | 45.61 | 72.64 | 60.06 | 62.03 |
| Qwen3-8B | BF16 | 55.38 | 83.50 | 86.73 | 57.12 | 76.50 | 67.88 | 71.19 | 55.38 | 83.50 | 86.73 | 57.12 | 76.50 | 67.88 | 71.19 |
| | GPTQ | 54.27 | 82.74 | 86.73 | 56.62 | <u>76.22</u> | 66.77 | 70.56 | 44.28 | 74.62 | 83.33 | 53.88 | 75.95 | 67.56 | 66.60 |
| | AWQ | <u>53.67</u> | <u>82.37</u> | <u>85.93</u> | <u>55.91</u> | 75.79 | 68.75 | <u>70.40</u> | 50.56 | 80.93 | 84.43 | 52.80 | 75.90 | 67.25 | 68.65 |
| | QUIP | 45.48 | 75.42 | 81.99 | 44.72 | 69.53 | 62.67 | 63.30 | 40.27 | 71.93 | 77.37 | 43.22 | 71.33 | 59.83 | 60.66 |
| | O(N) | 53.75 | 82.20 | 86.02 | 56.39 | <u>76.22</u> | 68.03 | 70.44 | <u>47.69</u> | 77.61 | 84.46 | 53.76 | 74.76 | 67.35 | 67.61 |
| | O(R) | 53.41 | 82.36 | 86.02 | 56.34 | <u>76.06</u> | <u>68.82</u> | 70.50 | <u>47.59</u> | <u>77.62</u> | 84.04 | 53.88 | 74.59 | <u>67.46</u> | 67.53 |
| | O | <u>54.18</u> | 82.62 | 86.45 | 55.70 | 76.39 | 68.59 | 70.66 | <u>47.27</u> | 78.41 | <u>84.39</u> | 54.23 | 76.27 | 67.90 | <u>68.08</u> |

Table 2: **Zero-shot accuracy comparison on six common sense reasoning tasks across Llama3-8B, Qwen3-4B, and Qwen3-8B.** The evaluation is conducted under **4-bit** and **3-bit** quantization settings. We denote our proposed methods as: **O(N)** for Naïve Babai, **O(R)** for Random K -Best Babai, and **O** for Random K -Best Babai with Joint Activation-Target optimization. The unquantized **BF16** baseline is shaded in gray. For quantized methods, **bold** indicates the best result and underlining denotes the second-best.

ated on LM-harness library [Gao *et al.*, 2024]

Perplexity Table 1 reports perplexity (PPL) across multiple LLaMA-2/3, Qwen-3, and Mistral models under group-wise weight-only quantization with activation precision fixed at 16-bit. At 4-bit, existing PTQ methods such as GPTQ and AWQ achieve reasonable performance on large LLaMA models but exhibit noticeable degradation or instability on harder architectures, particularly Qwen-0.6B and llama-3-8B, while RTN frequently diverges. In contrast, our method consistently attains the lowest or near-lowest perplexity across all model families, with clear improvements in challenging regimes. The advantage becomes more pronounced at 3-bit, where prior methods often suffer sharp performance drops or catastrophic failures, whereas our approach remains stable and shows smooth degradation relative to BF16. These results indicate that jointly optimizing quantization objectives and search strategies leads to substantially improved robustness under low-bit quantization, especially for smaller and more sensitive models. When group quantization is disabled (group size = 0), baseline methods such as GPTQ, AWQ, and QUIP exhibit a clear increase in quantization error, with substantial performance degradation and, in some cases, numerical instability—particularly for smaller and more sensitive models. In contrast, our method remains stable in this setting and consistently preserves low perplexity across all architectures.

Zero-shot accuracy Table 2 compares BF16 and low-bit PTQ methods across three model families under both 4-bit and 3-bit settings. At 4 bits, all methods remain relatively close to BF16, but our approach consistently achieves the strongest or second-strongest performance across most tasks and models, yielding the highest average accuracy for all three backbones. Notably, the gains are more pronounced on reasoning-heavy benchmarks such as ARC-C, ARC-E, and Hella, indicating improved robustness beyond simple lexical or pattern-matching tasks. When moving to the more challenging 3-bit regime, performance gaps widen substantially: GPTQ and QUIP exhibit significant degradation, particularly on ARC and Hella, while our method degrades more gracefully and maintains clear advantages in average performance. This trend is consistent across model scales, from Qwen-3-4B to Qwen-3-8B, suggesting that the proposed approach scales favorably and is less sensitive to aggressive quantization. Overall, the results demonstrate that our method not only preserves accuracy under moderate compression but also provides superior stability in extreme low-bit settings, highlighting its effectiveness as a general and robust PTQ solution.

Reasoning Table 3 reports reasoning accuracy on GSM8K, GPQA, and MBPP under 4-bit quantization across three model families. Compared to GPTQ, AWQ, and QUIP, our method consistently achieves the highest average accuracy for all backbones, with particularly strong gains on GSM8K

| Bit | Method | LLaMA3-8B | | | | Qwen3-4B | | | | Qwen3-8B | | | |
|-----------------|--------|--------------|--------------|--------------|--------------|--------------|--------------|--------------|--------------|--------------|--------------|--------------|--------------|
| | | GSM8K | GPQA | MBPP | Avg | GSM8K | GPQA | MBPP | Avg | GSM8K | GPQA | MBPP | Avg |
| BF16 | BF16 | 51.86 | 35.98 | 48.40 | 45.41 | 83.70 | 38.38 | 62.40 | 61.49 | 88.48 | 33.33 | 65.00 | 62.27 |
| 4-bit (g128) | GPTQ | 45.03 | 29.27 | 45.00 | 39.77 | 57.71 | 31.81 | 27.60 | 39.77 | 86.80 | 36.86 | 60.20 | 61.29 |
| | AWQ | 44.42 | <u>32.32</u> | 46.40 | 41.05 | 80.15 | 33.33 | 57.80 | 57.09 | 85.44 | 32.83 | 62.80 | 60.36 |
| | QUIP | 42.30 | 29.87 | 40.40 | 37.52 | 5.69 | 25.75 | 0.00 | 10.48 | 64.40 | 31.31 | 0.00 | 31.90 |
| | Ours | 48.22 | 32.93 | 44.80 | 41.98 | 84.29 | 36.36 | <u>56.80</u> | 59.15 | 87.87 | 34.34 | 63.20 | 61.80 |

Table 3: Reasoning accuracy (%) on GSM8K, GPQA, and MBPP benchmarks. We evaluate LLaMA3-8B, Qwen3-4B, and Qwen3-8B. All quantized methods are evaluated with 4-bit weights and a group size of 128 (g128). Our method (denoted as Ours) employs Random K Babai with Joint Target Activation (JTA) optimization. The unquantized baseline is reported in BF16. Bold indicates the best result and underlining denotes the second-best.

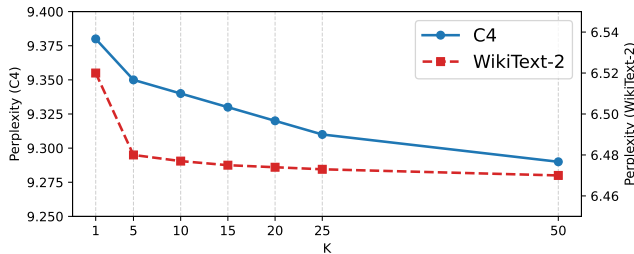


Figure 2: Ablation study on the candidate size K . We evaluate the perplexity on C4 and WikiText-2 datasets using Llama-3-8B with 4-bit quantization (group size 128). The results demonstrate the impact of increasing the search space K .

and GPQA, which require multi-step numerical and factual reasoning. While AWQ remains competitive on MBPP for some models, its performance is less consistent across tasks, leading to lower overall averages. QUIP exhibits severe degradation on reasoning benchmarks, including complete failure on MBPP for Qwen models, highlighting its instability under reasoning-intensive workloads. In contrast, our approach maintains balanced performance across arithmetic, knowledge-intensive, and program synthesis tasks, closely tracking BF16 accuracy despite aggressive quantization. These results indicate that the proposed method better preserves structured reasoning capabilities under low-bit constraints, rather than overfitting to a single task type or model family.

Ablations We investigate the impact of the hyperparameter K by varying it within $\{1, 5, \dots, 50\}$ under the setting of 4-bit Llama-3-8B with a group size of 128. As illustrated in Fig. 2, the perplexity on both WikiText-2 and C4 exhibits a significant drop at $K = 5$. Beyond this point, while the performance continues to improve up to $K = 50$, the marginal gains become negligible. Based on these observations, we select $K = 5$ as the default configuration for our method.

We analyze the impact of μ and λ on WikiText-2 in Fig. 3. For μ , performance is optimized at 0.6 but degrades at the boundaries (0.1, 1.0). This confirms that neither Eq. 1 nor Eq. 4 alone is sufficient; a balanced combination is essential. For λ , despite higher variance, setting $\lambda = 0.6$ yields a robust minimum. Consequently, we adopt $(\mu = 0.6, \lambda = 0.6)$ as the

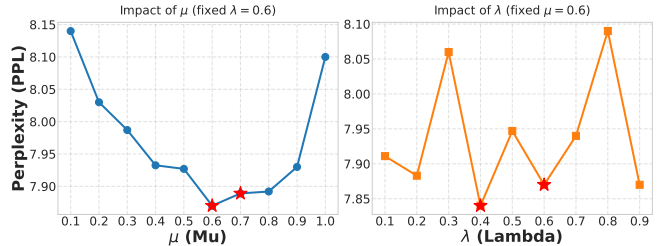


Figure 3: Sensitivity analysis of hyperparameters μ and λ . Evaluated on WikiText-2 (calibrated on C4), the plots show the perplexity trend when varying one parameter while fixing the other at 0.6. The U-shaped curve for μ (left) confirms the necessity of balancing the two objectives, while λ (right) shows 0.6 as a robust operating point.

default configuration for 3 bits setting. Similarly, we adopt $(\mu = 0.1, \lambda = 0.2)$ for 4 bits setting.

5 Conclusion

We presented a unified post-training quantization framework that reformulates layer-wise weight quantization as a structured integer optimization problem and solves it using a joint objective with Babai-type decoding. By integrating compensation-aware targets and controlled randomness, the proposed method consistently outperforms existing PTQ approaches across a wide range of models, tasks, and bit-widths. Extensive experiments on both general evaluation benchmarks and reasoning-intensive tasks demonstrate that our approach preserves accuracy more effectively under aggressive low-bit quantization, while remaining stable across model scales. These results suggest that principled optimization-based formulations provide a robust foundation for future low-bit quantization methods, bridging classical lattice decoding techniques and modern large language model compression.

Limitations Our current framework does not yet incorporate weight permutation (e.g., GPTQ) or dynamic scaling, which are promising for future integration. Additionally, we presently use fixed hyperparameters (μ, λ) and candidate size K for all layers. Future work will explore layer-wise adaptive strategies, specifically assigning distinct μ, λ and varying the number of random candidates per layer to better match the sensitivity of different model components.

References

- Josh Achiam, Steven Adler, Sandhini Agarwal, Lama Ahmad, Ilge Akkaya, Florencia Leoni Aleman, Diogo Almeida, Janko Altenschmidt, Sam Altman, Shyamal Anadkat, et al. Gpt-4 technical report. *arXiv preprint arXiv:2303.08774*, 2023.
- E. Agrell, T. Eriksson, A. Vardy, and K. Zeger. Closest point search in lattices. *IEEE Trans. Inf. Theory*, 48(8):2201–2214, 2002.
- Erik Agrell, Thomas Eriksson, Alexander Vardy, and Kenneth Zeger. Closest point search in lattices. *IEEE transactions on information theory*, 48(8):2201–2214, 2002.
- Yamato Arai and Yuma Ichikawa. Quantization error propagation: Revisiting layer-wise post-training quantization. In *The Thirty-ninth Annual Conference on Neural Information Processing Systems*, 2025.
- Jacob Austin, Augustus Odena, Maxwell Nye, Maarten Bosma, Henryk Michalewski, David Dohan, Ellen Jiang, Carrie Cai, Michael Terry, Quoc Le, and Charles Sutton. Program synthesis with large language models, 2021.
- László Babai. On lovász’ lattice reduction and the nearest lattice point problem. *Combinatorica*, 6(1):1–13, 1986.
- L. Bai, J. Choi, and Q. Yu. *Low Complexity MIMO Receivers*. Springer, Cham, Germany, 2014.
- Luis G Barbero and John S Thompson. Performance analysis of a fixed-complexity sphere decoder in high-dimensional MIMO systems. In *2006 IEEE International Conference on Acoustics Speech and Signal Processing Proceedings*, volume 4, pages IV–IV. IEEE, 2006.
- Yonatan Bisk, Rowan Zellers, Jianfeng Gao, Yejin Choi, et al. Piqa: Reasoning about physical commonsense in natural language. In *Proceedings of the AAAI conference on artificial intelligence*, volume 34, pages 7432–7439, 2020.
- X.-W. Chang, X. Yang, and T. Zhou. MLAMBDA: A modified LAMBDA method for integer least-squares estimation. *Journal of Geodesy*, 79(9):552–565, 2005.
- Xiao-Wen Chang, Qincheng Lu, and Yingzi Xu. Success probabilities of l2-norm regularized babai detectors and maximization. In *2023 IEEE International Symposium on Information Theory (ISIT)*, pages 1219–1224, 2023.
- Xiao-Wen Chang, Zhilong Chen, and Jinming Wen. An extended babai method for estimating linear model based integer parameters. *Econometrics and Statistics*, 29:238–251, 2024.
- Jerry Chee, Yaohui Cai, Volodymyr Kuleshov, and Christopher De Sa. Quip: 2-bit quantization of large language models with guarantees, 2024.
- Lingjiao Chen, Matei Zaharia, and James Zou. Frugalgpt: How to use large language models while reducing cost and improving performance. *arXiv preprint arXiv:2305.05176*, 2023.
- Jiale Chen, Yalda Shabanzadeh, Elvir Crnčević, Torsten Hoefler, and Dan Alistarh. The geometry of llm quantization: Gptq as babai’s nearest plane algorithm, 2025.
- Peter Clark, Isaac Cowhey, Oren Etzioni, Tushar Khot, Ashish Sabharwal, Carissa Schoenick, and Oyvind Tafjord. Think you have solved question answering? try arc, the ai2 reasoning challenge. *arXiv preprint arXiv:1803.05457*, 2018.
- Karl Cobbe, Vineet Kosaraju, Mohammad Bavarian, Mark Chen, Heewoo Jun, Lukasz Kaiser, Matthias Plappert, Jerry Tworek, Jacob Hilton, Reiichiro Nakano, Christopher Hesse, and John Schulman. Training verifiers to solve math word problems, 2021.
- Gheorghe Comanici, Eric Bieber, Mike Schaekermann, Ice Pasupat, Noveen Sachdeva, Inderjit Dhillon, Marcel Bliestein, Ori Ram, Dan Zhang, Evan Rosen, Luke Marri, Sam Petulla, Colin Gaffney, Asaf Aharoni, Nathan Lintz, Tiago Cardal Pais, Henrik Jacobsson, Idan Szpektor, Nan-Jiang Jiang, Krishna Haridasan, Ahmed Omran, Nikunj Saunshi, Dara Bahri, Gaurav Mishra, Eric Chu, Toby Boyd, Brad Hekman, Aaron Parisi, Chaoyi Zhang, Kornraphop Kawintiranon, Tania Bedrax-Weiss, Oliver Wang, Ya Xu, Ollie Purkiss, Uri Mendlovic, Ilai Deutel, Nam Nguyen, Adam Langley, Flip Korn, Lucia Rossazza, Alexandre Ramé, Sagar Waghmare, Helen Miller, Nathan Byrd, Ashrith Sheshan, Raia Hadsell, Sangnie Bhardwaj, Pawel Janus, Tero Rissa, Dan Horgan, Alvin Abdagic, Lior Belenki, James Allingham, Anima Singh, Theo Guidroz, Srivatsan Srinivasan, Herman Schmit, Kristen Chiafullo, Andre Elisseeff, Nilpa Jha, Prateek Kolhar, Leonard Berrada, Frank Ding, Xiance Si, Shrestha Basu Mallick, Franz Och, Sofia Errell, Eric Ni, Tejasi Latkar, Sherry Yang, Petar Sirkovic, Ziqiang Feng, Robert Leland, Rachel Hornung, et al. Gemini 2.5: Pushing the frontier with advanced reasoning, multimodality, long context, and next generation agentic capabilities, 2025.
- Elias Frantar, Saleh Ashkboos, Torsten Hoefler, and Dan Alistarh. Gptq: Accurate post-training quantization for generative pre-trained transformers, 2023.
- Leo Gao, Jonathan Tow, Baber Abbasi, Stella Biderman, Sid Black, Anthony DiPofi, Charles Foster, Laurence Golding, Jeffrey Hsu, Alain Le Noac’h, Haonan Li, Kyle McDonell, Niklas Muennighoff, Chris Ociepa, Jason Phang, Laria Reynolds, Hailey Schoelkopf, Aviya Skowron, Lintang Sutawika, Eric Tang, Anish Thite, Ben Wang, Kevin Wang, and Andy Zou. The language model evaluation harness, 07 2024.
- Aaron Grattafiori, Abhimanyu Dubey, Abhinav Jauhri, Abhinav Pandey, Abhishek Kadian, Ahmad Al-Dahle, Aiesha Letman, Akhil Mathur, Alan Schelten, Alex Vaughan, et al. The llama 3 herd of models, 2024.
- Albert Q. Jiang, Alexandre Sablayrolles, Arthur Mensch, Chris Bamford, Devendra Singh Chaplot, Diego de las Casas, Florian Bressand, Gianna Lengyel, Guillaume Lample, Lucile Saulnier, Léo Renard Lavaud, Marie-Anne Lachaux, Pierre Stock, Teven Le Scao, Thibaut Lavril, Thomas Wang, Timothée Lacroix, and William El Sayed. Mistral 7b, 2023.
- Philip Klein. Finding the closest lattice vector when it’s unusually close. In *Proceedings of the Eleventh Annual ACM-*

- SIAM Symposium on Discrete Algorithms*, SODA '00, page 937–941, USA, 2000. Society for Industrial and Applied Mathematics.
- Ji Lin, Jiaming Tang, Haotian Tang, Shang Yang, Wei-Ming Chen, Wei-Chen Wang, Guangxuan Xiao, Xingyu Dang, Chuang Gan, and Song Han. Awq: Activation-aware weight quantization for llm compression and acceleration, 2024.
- S. Liu, C. Ling, and D. Stehle. Decoding by sampling: A randomized lattice algorithm for bounded distance decoding. *IEEE Trans. Inf. Theor.*, 57(9):5933–5945, September 2011.
- Daniele Micciancio and Shafi Goldwasser. *Complexity of Lattice Problems: a cryptographic perspective*, volume 671 of *The Kluwer International Series in Engineering and Computer Science*. Kluwer Academic Publishers, Boston, Massachusetts, March 2002.
- Daniele Micciancio. The hardness of the closest vector problem with preprocessing. *IEEE Transactions on Information Theory*, 47(3):1212–1215, 2002.
- Colin Raffel, Noam Shazeer, Adam Roberts, Katherine Lee, Sharan Narang, Michael Matena, Yanqi Zhou, Wei Li, and Peter J Liu. Exploring the limits of transfer learning with a unified text-to-text transformer. *Journal of machine learning research*, 21(140):1–67, 2020.
- Colin Raffel, Noam Shazeer, Adam Roberts, Katherine Lee, Sharan Narang, Michael Matena, Yanqi Zhou, Wei Li, and Peter J Liu. Exploring the limits of transfer learning with a unified text-to-text transformer. *Journal of machine learning research*, 21(140):1–67, 2020.
- David Rein, Betty Li Hou, Asa Cooper Stickland, Jackson Petty, Richard Yuanzhe Pang, Julien Dirani, Julian Michael, and Samuel R. Bowman. Gpqa: A graduate-level google-proof q&a benchmark, 2023.
- Keisuke Sakaguchi, Ronan Le Bras, Chandra Bhagavatula, and Yejin Choi. Winogrande: An adversarial winograd schema challenge at scale. *Communications of the ACM*, 64(9):99–106, 2021.
- C. Schnorr and M. Euchner. Lattice basis reduction: improved practical algorithms and solving subset sum problems. *Math Program*, 66:181–191, 1994.
- Wenqi Shao, Mengzhao Chen, Zhaoyang Zhang, Peng Xu, Lirui Zhao, Zhiqian Li, Kaipeng Zhang, Peng Gao, Yu Qiao, and Ping Luo. Omniquant: Omnidirectionally calibrated quantization for large language models, 2024.
- P. J. G Teunissen. *GPS carrier phase ambiguity fixing concepts*. In Kleusberg A and Teunissen, P. J. G, editors, *GPS for Geodesy*, pp. 317–388. Springer, Heidelberg, 1996.
- Hugo Touvron, Thibaut Lavril, Gautier Izacard, Xavier Martinet, Marie-Anne Lachaux, Timothée Lacroix, Baptiste Rozière, Naman Goyal, Eric Hambro, Faisal Azhar, et al. Llama: Open and efficient foundation language models. *arXiv preprint arXiv:2302.13971*, 2023.
- Sergio Verdú. Computational complexity of optimum multiuser detection. *Algorithmica*, 4(3):303–312, 1989.
- Alex Wang, Yada Pruksachatkun, Nikita Nangia, Amanpreet Singh, Julian Michael, Felix Hill, Omer Levy, and Samuel Bowman. Superglue: A stickier benchmark for general-purpose language understanding systems. In H. Wallach, H. Larochelle, A. Beygelzimer, F. d'Alché-Buc, E. Fox, and R. Garnett, editors, *Advances in Neural Information Processing Systems*, volume 32. Curran Associates, Inc., 2019.
- Xinyu Wang, Vahid Partovi Nia, Peng Lu, Jerry Huang, Xiao-Wen Chang, Boxing Chen, and Yufei Cui. Potptq: A two-step power-of-two post-training for llms, 2025.
- Jinming Wen and Xiao-Wen Chang. On the success probability of three detectors for the box-constrained integer linear model. *IEEE Transactions on Communications*, 69(11):7180–7191, 2021. doi:10.1109/TCOMM.2021.3095127.
- An Yang, Anfeng Li, Baosong Yang, Beichen Zhang, Binyuan Hui, Bo Zheng, Bowen Yu, Chang Gao, Chengen Huang, Chenxu Lv, Chujie Zheng, Dayiheng Liu, et al. Qwen3 technical report, 2025.
- Rowan Zellers, Ari Holtzman, Yonatan Bisk, Ali Farhadi, and Yejin Choi. Hellaswag: Can a machine really finish your sentence? *arXiv preprint arXiv:1905.07830*, 2019.
- Jiaqi Zhao, Ming Wang, Miao Zhang, Yuzhang Shang, Xuebo Liu, Yaowei Wang, Min Zhang, and Liqiang Nie. Benchmarking post-training quantization in llms: Comprehensive taxonomy, unified evaluation, and comparative analysis, 2025.

A Appendix

Algorithm 2 Parallel K -Path Computation via Vectorized Back-Substitution

Require: Cholesky factor $\mathbf{R} \in \mathbb{R}^{m \times m}$, Continuous weights $\mathbf{W} \in \mathbb{R}^{m \times n}$

Require: Hyperparameters: K (candidates), B (block size)

Ensure: Candidate Integer Weights $\mathbf{Q} \in \mathbb{Z}^{(K) \times m \times n}$

- 1: **Initialization:**
 - 2: Initialize candidate centers $\mathbf{C} \in \mathbb{R}^{(K) \times m \times n}$ by broadcasting $\bar{\mathbf{W}}$
 - 3: Initialize \mathbf{Q} (storage for quantized values)
{Iterate backwards in blocks for matrix-level efficiency}
 - 4: **for** row block index $j_{start} = m$ **down to** 1 **step** B **do**
 - 5: Define current block $J = [j_{start} - B : j_{start}]$ and future block $F = [j_{start} : m]$
 - 6: **1. Global Vectorized Update (Matrix-Matrix Op)**
 - 7: **if** F is not empty **then**
 - 8: Compute quantization error from processed rows:
 $\Delta_F = \mathbf{C}_{:,F,:} - \mathbf{Q}_{:,F,:}$
 - 9: Propagate error to all K paths simultaneously using matrix multiplication:
 - 10: $\mathbf{C}_{:,J,:} \leftarrow \mathbf{C}_{:,J,:} + \frac{1}{\text{diag}(\mathbf{R})_J} (\mathbf{R}_{J,F} \cdot \Delta_F)$
 - 11: **end if**
 - 12: **2. Local Parallel Quantization**
 - 13: **for** row i from j_{start} **down to** $j_{start} - B$ **do**
 - 14: Update center $c_{:,i}$ using local neighbors within block J
 - 15: **Path Diversification (Vectorized Operation):**
 - 16: Path 0 (Greedy): $\mathbf{q}_{0,i} \leftarrow \text{Round}(c_{0,i})$
 - 17: Path 1.. K (Stochastic): $\mathbf{q}_{k,i} \leftarrow \text{Sample}(c_{k,i}, \text{top-}K)$
 - 18: **end for**
 - 19: **end for**
 - 20: **return** \mathbf{Q}
-

We record the per-layer quantization time on LLaMA3-8B for different values of K . Figure 4 reports the relative increase in layer-wise computation time under the K-best strategy.

As shown in Fig. 4, even when using $K = 25$ —corresponding to 25 independent randomized decoding paths—the additional computational overhead is modest, amounting to approximately an 80% increase in per-layer runtime. It suggests the usefulness of our parallelized algorithm

Table 4 presents an ablation over the hyperparameters μ and λ on WikiText-2. We observe that intermediate values of both parameters consistently yield lower perplexity, while overly small or large settings degrade performance. Although the global minimum is attained at $(\mu = 0.6, \lambda = 0.4)$, the configuration $(\mu = 0.6, \lambda = 0.6)$ achieves comparable performance (PPL 7.87) and lies within a stable low-perplexity region. For this reason, we fix $\mu = 0.6$ and $\lambda = 0.6$ in all main experiments, as it provides a robust trade-off without relying on the single best hyperparameter combination.

Algorithm 3 Quantization with JTA with random

- 1: Compute \mathbf{s} and \mathbf{z}
 - 2: Compute the Cholesky factorization: $\tilde{\mathbf{X}}^\top \tilde{\mathbf{X}} + \lambda^2 \mathbf{I} = \mathbf{R}^\top \mathbf{R}$
 - 3: Solve the lower triangular system $\mathbf{R}^\top \mathbf{u} = \mathbf{A}^\top \mathbf{y}$ and the upper triangular system $\mathbf{R} \mathbf{v} = \mathbf{u}$.
 - 4: Compute $\bar{\mathbf{q}} = \mathbf{v} \odot \mathbf{s} + \mathbf{z}$
 - 5: Compute $\bar{\mathbf{R}} = \mathbf{R} \mathbf{D}$
 - 6: $\mathbf{c}(m) = \hat{\mathbf{q}}(m)$
 - 7: $\Pr(\mathbf{q}_m = v) = \frac{\exp(-\alpha \bar{\mathbf{R}}_{ii} (\mathbf{c}_m - v)^2)}{\sum_{u=0}^{|\mathbb{B}|} \exp(-\alpha \bar{\mathbf{R}}_{ii} (\mathbf{c}_i - u)^2)}$, $v \in \mathbb{B}$
 - 8: **for** $i = m - 1 : -1 : 1$ **do**
 - 9: $\mathbf{c}(i) = \bar{\mathbf{q}}(i) + \left(\sum_{j=i+1}^m \bar{\mathbf{R}}(i, j) (\bar{\mathbf{q}}(j) - \mathbf{q}(j)) \right) / \bar{\mathbf{R}}(i, i)$
 - 10: $\Pr(\mathbf{q}_i = v) = \frac{\exp(-\alpha \bar{\mathbf{R}}_{ii} (\mathbf{c}_i - v)^2)}{\sum_{u=0}^{|\mathbb{B}|} \exp(-\alpha \bar{\mathbf{R}}_{ii} (\mathbf{c}_i - u)^2)}$, $v \in \mathbb{B}$
 - 11: **end for**
-

Algorithm 4 K-Best Randomized JTA Quantization

Require: Input matrices $\tilde{\mathbf{X}}, \mathbf{y}, \mathbf{W}$, regularization λ , bit-width wbit , number of trials K

Ensure: Quantized vector \mathbf{q}^*

- 1: Initialize best residual $r^* \leftarrow +\infty$
 - 2: Initialize $\mathbf{q}^* \leftarrow \mathbf{0}$
 - 3: **for** $k = 1$ to K **do**
 - 4: Run Algorithm 3 to obtain a candidate $\mathbf{q}^{(k)}$
 - 5: Compute residual
- $$r^{(k)} = \left\| \mathbf{A} \mathbf{D} \mathbf{q}^{(k)} - \mathbf{b} \right\|_2^2$$
- 6: **if** $r^{(k)} < r^*$ **then**
 - 7: $r^* \leftarrow r^{(k)}$
 - 8: $\mathbf{q}^* \leftarrow \mathbf{q}^{(k)}$
 - 9: **end if**
 - 10: **end for**
 - 11: **return** \mathbf{q}^*
-

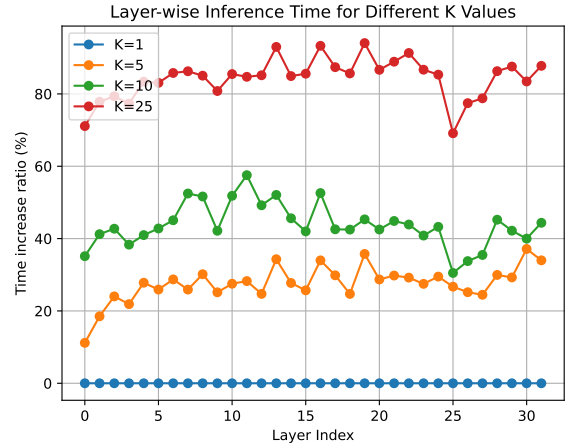


Figure 4: Layer Time increase ratio for different K on Llama3-8B 4 bits

Table 4: Perplexity on WikiText-2 for LLaMA-3-8B under different (μ, λ) and 3 bits settings. Lower is better.

| $\mu \backslash \lambda$ | 0.1 | 0.2 | 0.3 | 0.4 | 0.5 | 0.6 | 0.7 | 0.8 |
|--------------------------|--------|--------|--------|---------------|--------|--------|--------|---------------|
| 0.1 | 8.2499 | 8.1392 | 8.0821 | 8.0682 | 8.0099 | 8.0259 | 8.0285 | 8.0134 |
| 0.2 | 8.1045 | 8.0339 | 7.9979 | 7.9550 | 7.9797 | 7.9594 | 7.9868 | 7.9749 |
| 0.3 | 7.9992 | 7.9873 | 7.9506 | 7.9348 | 7.9198 | 7.9590 | 8.0508 | 7.9643 |
| 0.4 | 7.9634 | 7.9326 | 7.8940 | 7.9097 | 7.8870 | 7.9471 | 8.0463 | 7.8804 |
| 0.5 | 7.9515 | 7.9277 | 7.8604 | 7.8695 | 8.0539 | 7.8604 | 8.1135 | 7.9339 |
| 0.6 | 7.9111 | 7.8839 | 8.0664 | 7.8404 | 7.9041 | 7.8726 | 8.0893 | 7.8665 |
| 0.7 | 7.9198 | 7.8892 | 7.8613 | 7.8656 | 7.8874 | 7.8443 | 8.3100 | 8.2792 |
| 0.8 | 7.9172 | 7.8927 | 7.9665 | 7.9049 | 7.8874 | 7.8905 | 8.4475 | 8.3451 |
| 0.9 | 8.0570 | 7.9295 | 7.9815 | 7.9594 | 7.9616 | 8.0790 | 8.5767 | – |
| 1.0 | 8.2239 | 8.1054 | 8.1319 | 8.1207 | 8.0602 | 8.0781 | 8.8646 | – |